International Journal of Advanced Engineering and Technology Research
ISSN: 3106-8677 (Print), ISSN: 3106-8685 (Online) | Vol. 1, No. 3, 2026

Fabrication and Performance Tuning of Silica/Silicone Rubber Composites for High-Permittivity Low-Modulus Dielectric Elastomers

Xianxu Luo [1], Wen Huang [1] and Yuhao Wang [1, 2, *]

[1] Beijing University of Chemical Technology, Beijing 100029, China
[2] Beijing Xinfeng Aerospace Equipment Co. Ltd, Beijing, 100854, China

Abstract: Dielectric elastomers (DEs) are promising electroactive polymers owing to their low modulus, large actuation strain, and fast response. Silicone rubber, particularly polymethylvinylsiloxane (PMVS), is highly attractive due to its excellent flexibility and fatigue resistance. However, its low dielectric constant limits electromechanical performance. Here, we report a synergistic strategy that combines KH570-modified SiO_2 nanoparticles with tunable liquid-to-solid PMVS ratios. By optimizing the matrix composition, the SiO_2@3L7S composite (liquid:solid = 3:7) achieves an optimal balance of high dielectric constant and low modulus. The dielectric constant reaches 4.0 (46% higher than pure PMVS), while the maximum actuation strain increases to 45.4%—50% higher than the solid PMVS baseline—delivering a high energy density of 20.5 mJ/g. This approach, integrating covalent interfacial bonding and homologous plasticization, offers a simple yet effective route to high-performance silicone-based dielectric elastomer actuators for soft robotics and artificial muscles.

Keywords: Dielectric elastomer actuator, Dielectric elastomer, SiO_2 nanoparticles, Dielectric constant, Electromechanical strain, Energy density.

1. Introduction

Dielectric elastomer actuators (DEAs) have emerged as promising candidates for soft robotics, artificial muscles, flexible optics, and haptic feedback systems [1–4], owing to their large strains, high energy density, fast response times, and muscle-like compliance [5, 6]. As illustrated in Fig. 1, a DEA consists of a thin elastomer film sandwiched between two compliant electrodes [7, 8]. In the deactivated state (a), the material remains undeformed. Upon applying an electric field (b), opposite charges accumulate on the electrodes, generating Maxwell stress that compresses the film in thickness and expands it in area, thereby converting electrical energy into mechanical work [9].

The actuation performance is governed by the Maxwell stress equation, in which the electro-induced strain scales with the relative dielectric permittivity (ε_r) and the square of the applied electric field, while being inversely proportional to the Young's modulus (Y) [10–13]. Conventional silicone-based elastomers, such as polydimethylsiloxane (PDMS) and polymethylvinylsiloxane (PMVS), exhibit intrinsically low ε_r (≈2.5–3.0), which necessitates high driving voltages and limits practical applications [14, 15].

A common approach to increase dielectric permittivity is to incorporate high-permittivity ceramic fillers, such as SiO_2 nanoparticles, into the silicone rubber matrix [16–18]. However, unmodified SiO_2 tends to agglomerate and shows poor interfacial compatibility with the organic matrix, resulting in increased Young's modulus and reduced breakdown strength [19–23]. Although surface functionalization has yielded partial improvements, simultaneously achieving high permittivity, low modulus, and high breakdown strength remains challenging [11, 21, 22].

This work addresses these limitations through a synergistic strategy: covalent grafting of the silane coupling agent KH570 onto SiO_2 surfaces to enhance interfacial bonding, combined with precise tuning of the liquid-to-solid PMVS ratio to reduce modulus while maintaining processability. The optimal SiO_2@3L7S composite (liquid: solid = 3:7) effectively balances high dielectric constant and low Young's modulus, delivering significantly enhanced electromechanical performance [4, 13, 21].

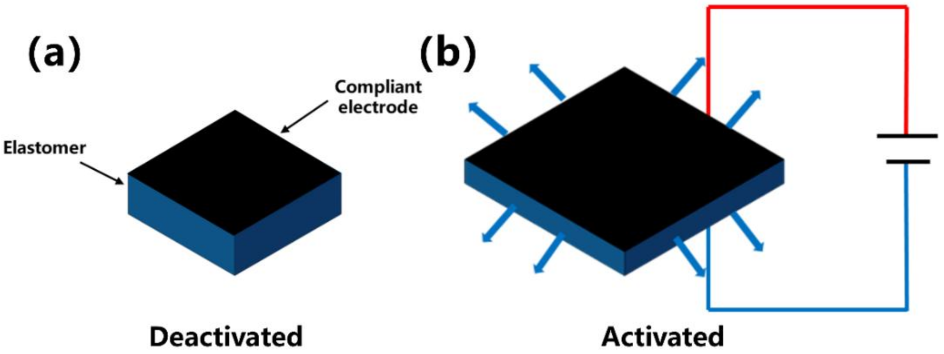

Figure 1. Operating principle of a dielectric elastomer actuator (DEA). (a) Deactivated state without applied voltage; (b) Activated state under applied electric field, where Maxwell stress causes thickness compression and in-plane expansion

2. Results and Discussion

2.1. Materials and Methods

The principal experimental parameters, including a KH570 concentration of 5 wt%, a filler loading of 7.5 phr, and a dicumyl peroxide (DCP) content of 0.5 phr, were established through preliminary optimization studies to achieve effective surface functionalization, homogeneous filler dispersion, and robust crosslinking.

Fig. 2. illustrates Pristine SiO_2 was dispersed in a 5 wt% ethanol solution of γ-methacryloxypropyltrimethoxysilane (KH570) and homogenized with a high-speed mixer for 5 min. The suspension was subsequently dried in a vacuum oven at 80 °C for 2 h to evaporate the solvent and facilitate silane grafting onto the particle surface. The particles were then washed three times with ethanol to remove unreacted KH570 and residual impurities, followed by further vacuum drying at 80 °C for 2 h, yielding chemically stable surface-modified SiO_2 fillers.

For composite preparation, solid and liquid PMVS were first blended at solid-to-liquid mass ratios of 9:1, 8:2, 7:3, and 6:4 (Table 1). Subsequently, 7.5 phr of the KH570-modified SiO_2 particles were incorporated by two-roll milling for 20 min to promote uniform dispersion and strong interfacial adhesion. Next, 0.5 phr DCP was added as the vulcanizing agent, and mixing was continued for an additional 10 min to ensure homogeneous distribution. The compounded mixtures were molded into films of 0.10 ± 0.01 mm thickness and vulcanized by hot pressing at 160 °C under 15 MPa for 10 min to accomplish complete crosslinking. After curing, the specimens were demolded and designated SiO_2@nL(10−n)S, where nL(10−n)S denotes the liquid-to-solid mass ratio of PMVS (e.g., SiO_2@1L9S corresponds to a solid-to-liquid ratio of 9:1). All procedures were performed in triplicate to guarantee reproducibility.

Table 1. Experimental formulation of SiO_2/PMVS composites

Specimen name	PMVS	PMVS solid-liquid ratio	SiO_2	DCP
SiO_2@1L9S	100	9:1	7.5	0.5
SiO_2@2L8S	100	8:2	7.5	0.5
SiO_2@3L7S	100	7:3	7.5	0.5
SiO_2@4L6S	100	6:4	7.5	0.5

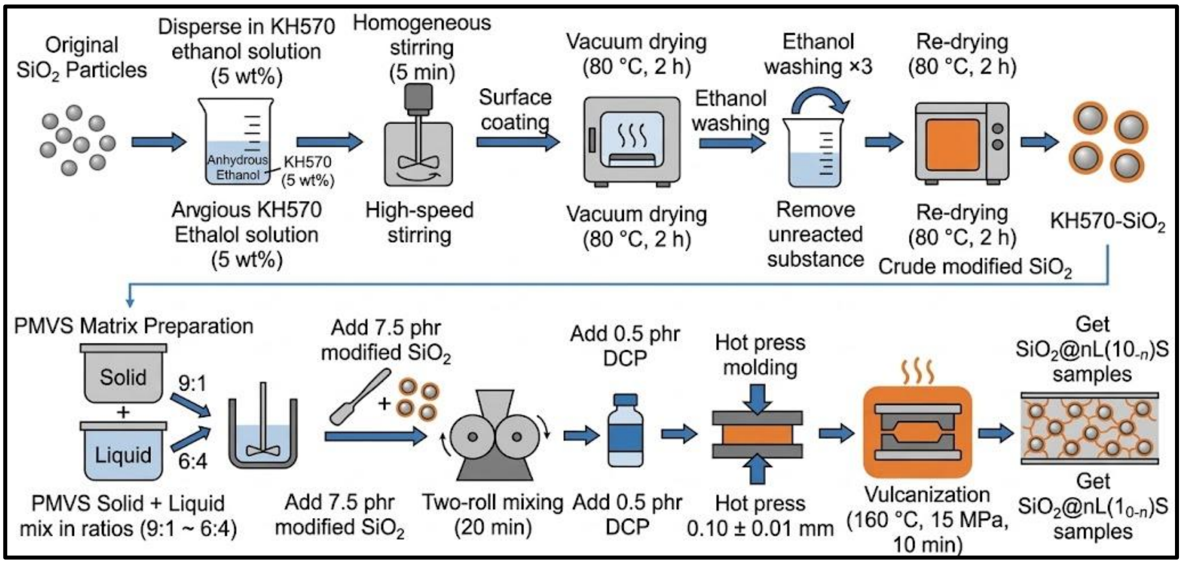

Figure 2. Flow chart for the preparation of KH570 modified SiO_2/PMVS composites

2.2. Molecular Modification and Microstructural Characterization

This study addresses the longstanding bottleneck in traditional SiO_2-filled silicone rubber dielectric elastomers. Unmodified SiO_2 nanoparticles are prone to agglomeration within the polymethylvinylsiloxane (PMVS) matrix owing to their intrinsically high surface energy. Moreover, the abundant surface hydroxyl groups on unmodified SiO_2 directly participate in the cross-linking reaction of the PMVS matrix, markedly increasing cross-linking density, chain rigidity, and Young's modulus. This inherent incompatibility prevents conventional filled systems from simultaneously achieving high dielectric permittivity and low modulus, thereby severely limiting electro-induced actuation performance and the practical applicability of dielectric elastomer actuators (DEAs).

To overcome this performance paradox, the present work introduces a dual-regulation strategy that integrates interfacial engineering of SiO_2 nanofillers with precise modulation of cross-linked network flexibility in the PMVS matrix. As depicted in Fig. 3. (a), the methoxy groups ($-OCH_3$) of the silane coupling agent KH570 (denoted as CA) undergo dealcoholization condensation ($-CH_3OH$ release) with the surface hydroxyl groups of SiO_2 at elevated temperature. This reaction enables stable covalent grafting of CA onto the SiO_2 surface, forming SiO_2@CA particles in which one end of the CA molecule is anchored via Si–O–Si bonds while the methacryloxy double bond remains available for co-crosslinking with the PMVS network (cyan structure shown on the right).

Fig. 3. (b) further illustrates the hierarchical design of the composite system. Starting from the pure PMVS network, unmodified SiO_2 nanoparticles are first incorporated to form the SiO_2/PMVS composite. Subsequent addition of the KH570 coupling agent produces the final CA@SiO_2/SiR architecture, in which the grafted CA molecules (highlighted by red circles) establish strong covalent bridges between the inorganic fillers and the organic matrix. Building upon this CA-modified SiO_2, the solid-to-liquid ratio of the PMVS matrix is precisely tuned (optimal at 7:3 in SiO_2@3L7S) to regulate cross-linking density and network flexibility. The

incorporation of liquid PMVS reduces chain rigidity and Young's modulus while maintaining excellent processability and filler dispersion.

This dual-regulation strategy—covalent interfacial bonding combined with homologous plasticization—harmonizes three core performance parameters required by high-performance DEAs: enhanced dielectric permittivity from interfacial polarization at the SiO_2 fillers, significantly lowered Young's modulus through flexible network regulation, and preserved high electrical breakdown strength ensured by robust filler–matrix interactions. Consequently, the approach transcends conventional performance trade-offs and establishes a novel materials-design paradigm for fabricating silicone-based DEAs with superior comprehensive electromechanical properties.

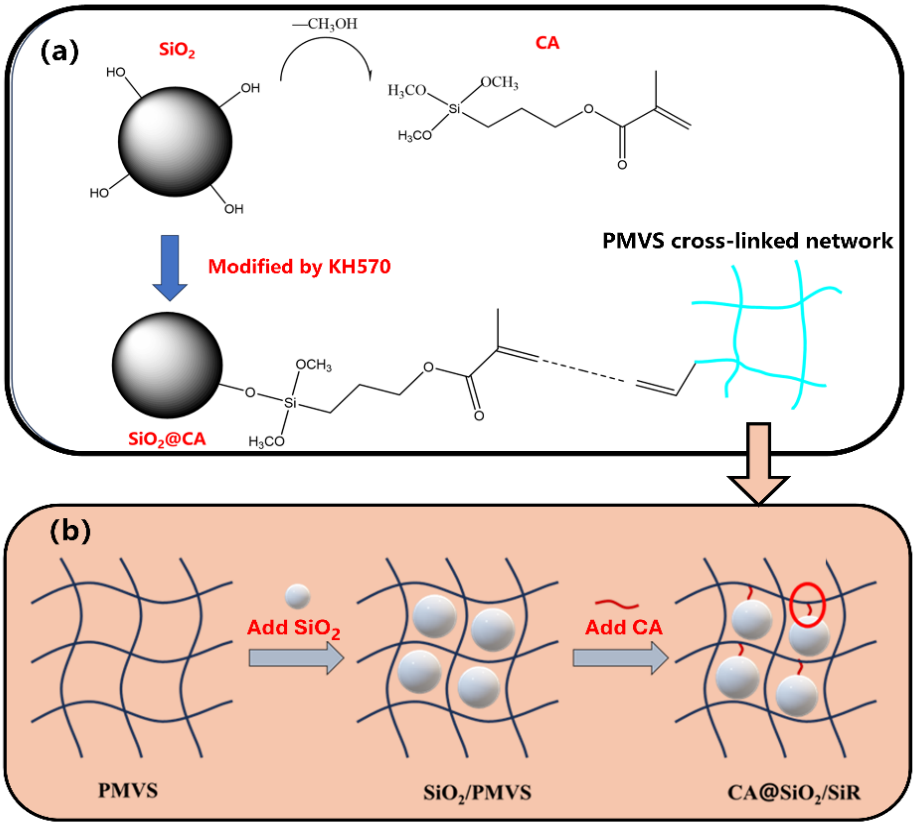

Figure 3. Schematic illustration of the dual-regulation strategy for preparing high-performance SiO_2/PMVS dielectric elastomer composites. (a) Surface modification mechanism of SiO_2 nanoparticles with the silane coupling agent KH570 (CA): dealcoholization condensation reaction between methoxy groups of KH570 and surface hydroxyl groups of SiO_2, followed by co-crosslinking of the methacryloxy double bond with the PMVS network. (b) Hierarchical assembly process of the composite: incorporation of SiO_2 into the PMVS matrix and subsequent introduction of KH570 to form strong covalent interfacial bonding (highlighted by red circles) between the filler and matrix

Successful grafting of the silane coupling agent (CA, KH570) onto the SiO_2 surface is confirmed in Fig. 4(e, f), which provides the molecular foundation for robust filler–matrix interfacial interactions. In the FTIR spectrum (Fig. 4(e)), the intense –OH stretching vibration at 3450 cm^{-1} observed in pure SiO_2 is markedly attenuated after modification, indicating that the methoxy groups of KH570 have replaced a large fraction of the surface hydroxyl groups via dealcoholization condensation. Concurrently, two new characteristic bands appear at 1710 cm^{-1} (C=O stretching) and ~1630 cm^{-1} (C=C stretching), directly evidencing the covalent attachment of the methacryloxy-containing CA molecule onto the SiO_2 surface.

Quantitative verification is provided by the TGA thermograms in Fig. 4(f). Below 120 °C, the modified SiO_2 exhibits lower weight loss than pure SiO_2, consistent with the reduced content of physisorbed and chemisorbed water after hydroxyl substitution. Above 120 °C, the greater weight loss of the modified sample arises from thermal decomposition of the grafted CA layer, corresponding to a grafting ratio of 1.89 wt%. These complementary FTIR and TGA results confirm the formation of stable covalent SiO_2@CA particles.

The impact of PMVS solid-to-liquid ratio on filler dispersion is revealed in the cross-sectional SEM images (Fig. 4(a–d)). At a high solid content (SiO_2@1L9S, Fig. 4(a)), the SiO_2 nanoparticles are uniformly dispersed throughout the PMVS matrix with consistent inter-particle spacing and negligible agglomeration. With moderate liquid PMVS incorporation (SiO_2@2L8S and SiO_2@3L7S, Fig. 4(b,c)), excellent dispersion is maintained, showing only sparse, small agglomerates while the majority of fillers remain individually distributed. In sharp contrast, further increasing the liquid PMVS fraction to 6:4 (SiO_2@4L6S, Fig. 4(d)) induces severe filler agglomeration and localized clusters. These microstructural changes directly correlate with the macroscopic mechanical, dielectric, and electromechanical properties, demonstrating that the optimal 3:7 solid-to-liquid ratio (SiO_2@3L7S) achieves the best balance of dispersion, interface quality, and network flexibility.

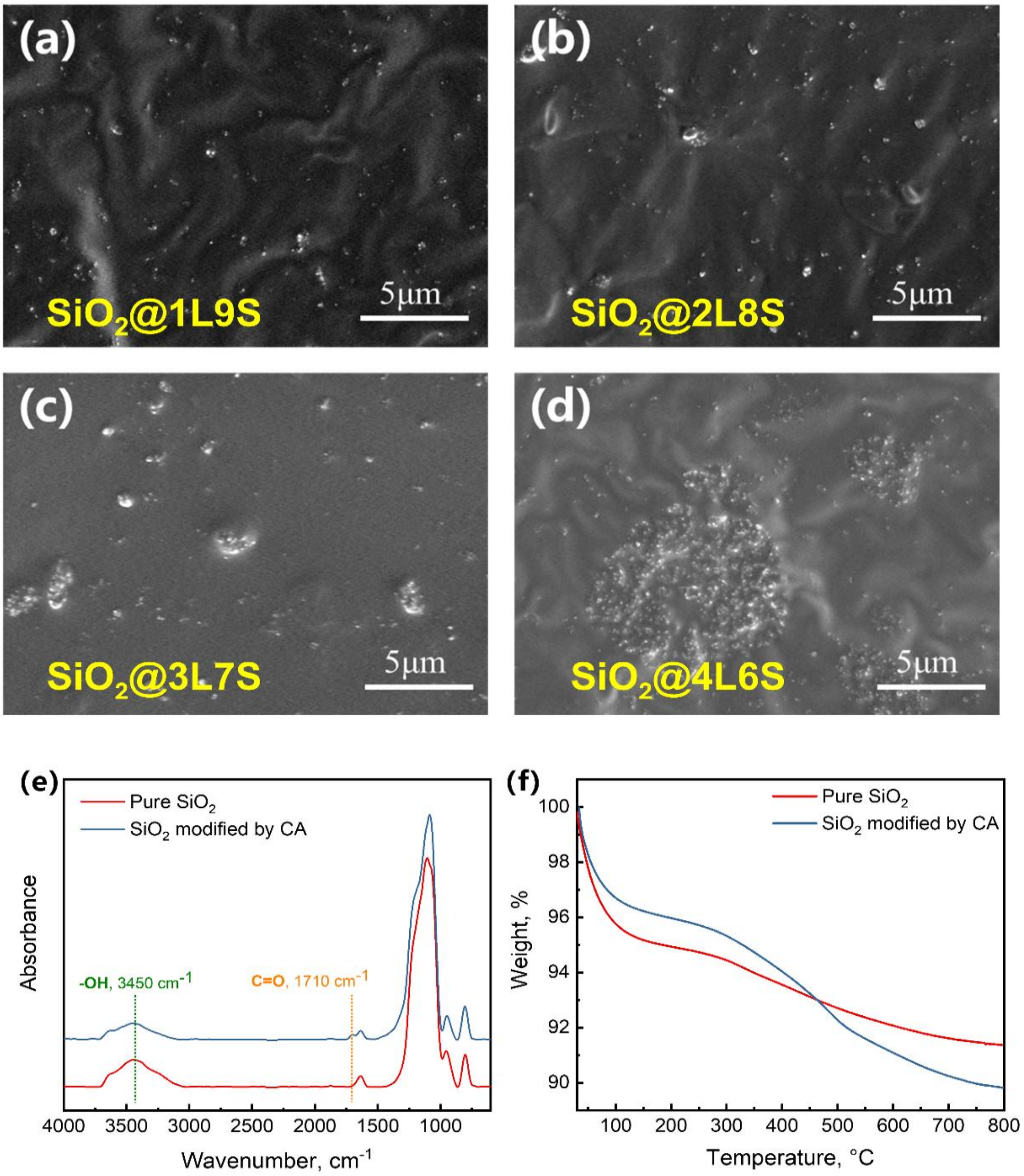

Figure 4. Characterization of KH570-modified SiO_2 nanoparticles and the effect of PMVS solid-to-liquid ratio on composite microstructure. (a–d) Cross-sectional SEM images of the SiO_2/PMVS composites with different solid-to-liquid PMVS ratios: (a) SiO_2@1L9S, (b) SiO_2@2L8S, (c) SiO_2@3L7S, and (d) SiO_2@4L6S (scale bar = 5 μm). (e) FTIR spectra and (f) TGA curves of pure SiO_2 (red) and CA-modified SiO_2 (blue)

2.3. Fundamental Electromechanical Properties

The mechanical properties of the composites, which critically govern electro-induced strain according to Maxwell stress theory, are presented in Fig. 5(a, b). As shown in the stress–strain curves (Fig. 5(a)), the tensile strength decreases gradually with increasing liquid PMVS content. More importantly, Young's modulus (Fig. 5(b)) declines continuously from 0.58 MPa for the pure solid PMVS composite (SiO_2@10S) to 0.24 MPa for SiO_2@3L7S (solid-to-liquid ratio 7:3), corresponding to a substantial 58.6% reduction. This softening effect arises from the reduced cross-linking density and enhanced chain mobility introduced by the liquid PMVS component.

The dielectric properties are displayed in Fig. 5(c–e). All SiO_2-filled composites exhibit significantly enhanced dielectric permittivity (ε_r) compared with the unfilled PMVS matrix (Fig. 5(c)). At low frequencies (10^{-1} Hz), the dielectric constant reaches 4.5 for SiO_2@10S and remains approximately 4.0 across the liquid-containing samples, representing a ~46% improvement over pure PMVS. Meanwhile, the dielectric loss tangent (tan δ) stays extremely low (< 0.1) over the entire frequency range (Fig. 4(d)), with values below 0.05 at higher frequencies for all formulations. The electrical conductivity (Fig. 5(e)) of all composites remains on the order of 10^{-13}–10^{-14} S/cm at low frequencies, confirming excellent insulating behavior.

The electrical breakdown performance is evaluated using Weibull statistics in Fig. 5(f). The characteristic breakdown strength (E_0) decreases moderately from 71 kV/mm for SiO_2@10S to 55 kV/mm for SiO_2@4L6S, while the shape parameter (β) remains relatively high, indicating good reliability. Comprehensive analysis of these results reveals that the SiO_2@3L7S composite (solid-to-liquid ratio 7:3) successfully breaks the traditional trade-off between dielectric permittivity and mechanical compliance, simultaneously providing high ε_r, significantly reduced Young's modulus, and maintained breakdown strength.

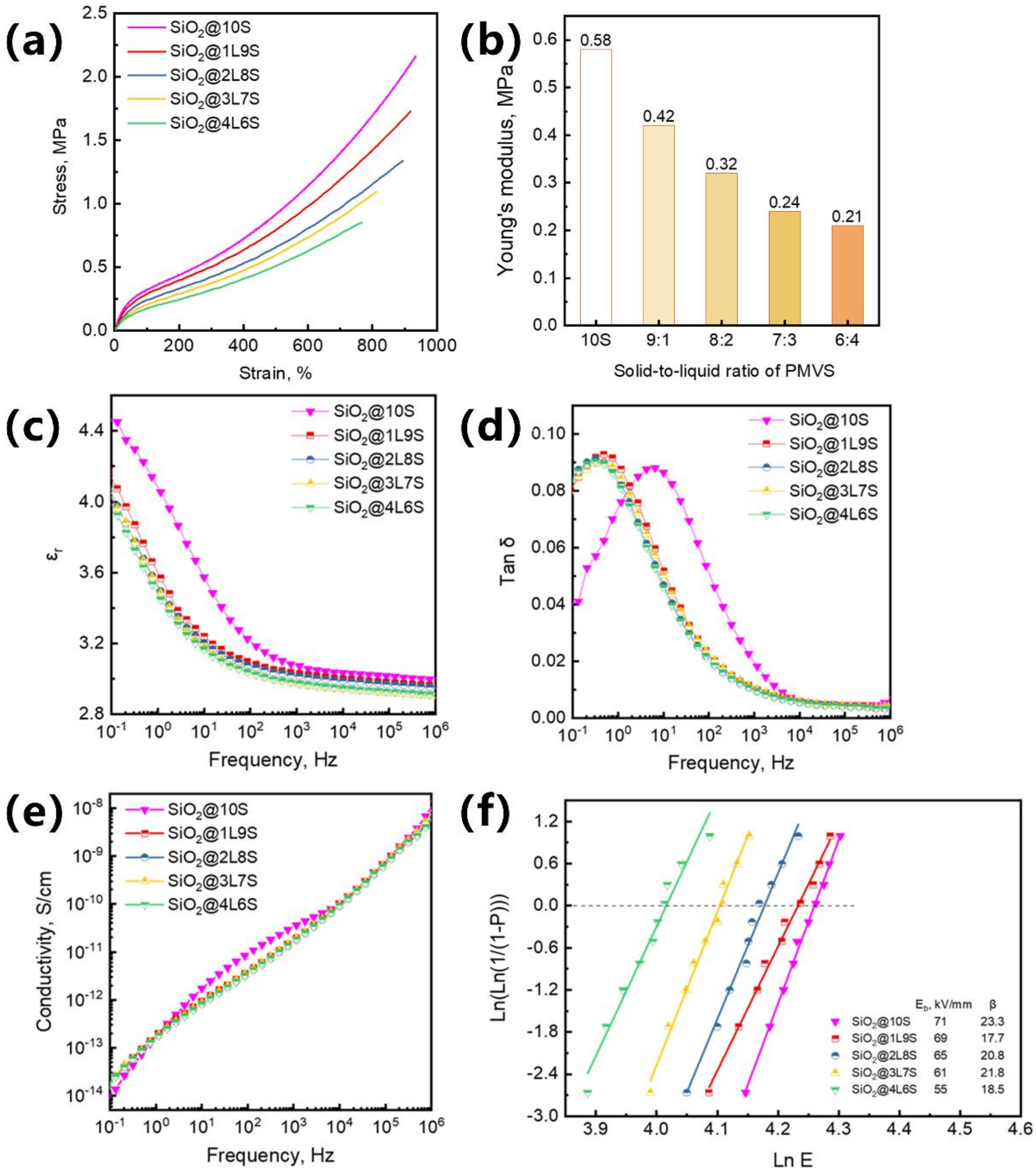

Figure 5. Mechanical, dielectric, and electrical breakdown properties of SiO_2/PMVS composites with different solid-to-liquid PMVS ratios. (a) Representative stress–strain curves; (b) Young's modulus as a function of solid-to-liquid ratio; (c) frequency-dependent dielectric constant (ε_r), (d) dielectric loss tangent (tan δ); (e) electrical conductivity; (f) Weibull plots of electrical breakdown strength (Eb) with characteristic breakdown strength (E_0) and shape parameter (β) values

As shown in Fig. 6a, the electromechanical sensitivity of the composites was evaluated based on the classical Maxwell stress theory. According to this theory, the electro-induced strain (s) of a dielectric elastomer actuator (DEA) is given by:

$$s = \varepsilon_0\ \varepsilon_r\ E^2 / Y \qquad (1)$$

where ε_0 is the permittivity of free space, ε_r is the relative permittivity, E is the applied electric field, and Y is the Young's modulus. Both the relative permittivity normalized by Young's modulus (ε_r/Y) and the squared term ($\varepsilon_r\ E_0^2/Y$, where E_0 represents a reference field) increase with increasing liquid PMVS content. These values reach their maximum at the solid-to-liquid ratio of 7:3 (SiO_2@3L7S), with $\varepsilon_r/Y = 19.5$ and $\varepsilon_r E_0^2/Y \approx 62963$, before decreasing sharply at the 6:4 ratio (SiO_2@6:4).

Fig 6 (b–d) present the directly measured actuation performance of the composites under increasing applied electrical fields. In Fig. 5b, the actuated area strain rises nonlinearly with the electric field for all samples. The SiO_2@3L7S composite exhibits the highest actuation performance, achieving a maximum areal strain of 45.4% at 55 kV/mm. Similarly, the blocked stress (Fig. 5c) and energy density (Fig. 5d) also increase with the applied field, with SiO_2@3L7S delivering the superior values of 61.2 kPa and 20.5 mJ g^{-1}, respectively, at high electric fields. In contrast, the SiO_2@4L6S composite shows noticeably lower blocked stress across the entire field range.

Collectively, the results in Fig. 5 demonstrate that the SiO_2@3L7S formulation achieves the optimal balance between high electromechanical sensitivity, large actuated strain, high blocked stress, and high energy density, making it the most promising candidate for high-performance dielectric elastomer actuators.

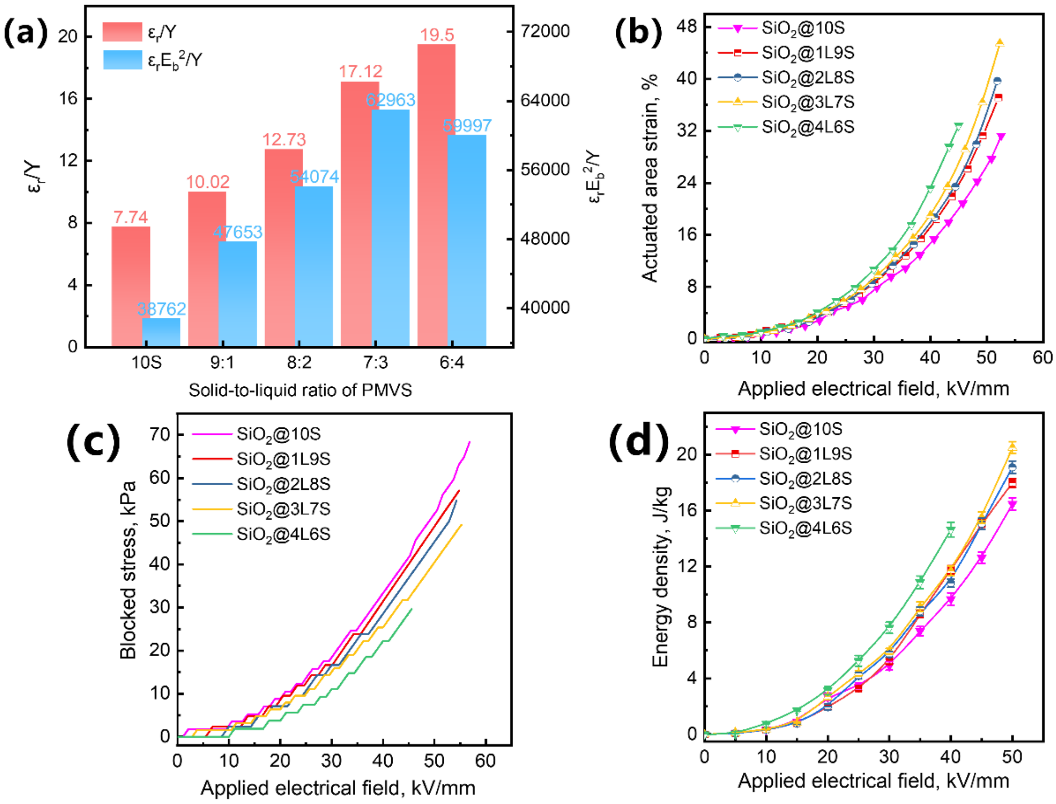

Figure 6. (a) Electromechanical sensitivity of the composites with different PMVS solid-to-liquid ratios; (b) Areal actuated strain as a function of applied electric field; (c) Blocked stress as a function of applied electric field; (d) Energy density as a function of applied electric field

3. Summary

In summary, this study demonstrates a straightforward and efficient dual-regulation strategy that synergistically combines KH570-mediated surface modification of SiO_2 nanoparticles with precise control of the solid-to-liquid PMVS ratio in the elastomer matrix. Covalent grafting of the silane coupling agent KH570 onto SiO_2 surfaces, as evidenced by attenuated –OH signals and the emergence of characteristic C=O and C=C bands in FTIR spectra alongside a grafting ratio of 1.89 wt% determined by TGA, establishes robust Si–O–Si interfacial bonding. This bonding significantly enhances filler–matrix compatibility and enables co-crosslinking within the PMVS network. Simultaneously, the incorporation of liquid PMVS as a homologous plasticizer reduces crosslinking density and chain rigidity, resulting in a substantial decrease in Young's modulus from 0.58 MPa (SiO_2@10S) to 0.24 MPa (SiO_2@3L7S), corresponding to a 58.6% reduction, while preserving processability and uniform filler dispersion. At the optimal solid-to-liquid ratio of 7:3 (SiO_2@3L7S), the composite exhibits a dielectric constant of approximately 4.0 (46% higher than that of pure PMVS), low dielectric loss (tan δ < 0.1 across the measured frequency range), and retained electrical breakdown strength. These improvements yield superior electromechanical performance, with a maximum electromechanical sensitivity (ε_r/Y) of 19.5, in accordance with classical Maxwell stress theory ($s = \varepsilon_0\varepsilon_r E^2/Y$). Under an applied electric field, the SiO_2@3L7S composite achieves an areal actuated strain of 45.4% at 55 kV/mm—approximately 50% higher than the solid PMVS baseline—along with a blocked stress of 61.2 kPa and an energy density of 20.5 mJ g^{-1}, outperforming other formulations. SEM analysis confirms uniform SiO_2 dispersion with minimal agglomeration up to the 3:7 ratio, whereas excessive liquid PMVS (6:4) induces filler clustering and performance degradation. Collectively, this approach effectively resolves the inherent trade-off between elevated dielectric permittivity and low elastic modulus in silica/silicone systems through enhanced interfacial polarization and modulated network flexibility. The strategy provides a robust, scalable materials-design framework for high-performance silicone-based dielectric elastomer actuators, positioning the SiO_2@3L7S composite as a new benchmark for nano-SiO_2-filled silicone DEAs in actuated strain and energy density, with promising applications in soft robotics, artificial muscles, flexible electronics, and energy-harvesting devices.

References

[1] Gu G, Zou J, Zhao R, et al. Soft wall-climbing robots [J]. Science Robotics, 2018, 3(25): eaat2874.

[2] O'Halloran A, O'Malley F, McHugh P. A review on dielectric elastomer actuators, technology, applications, and challenges [J]. Journal of Applied Physics, 2008, 104(7): 071101.

[3] Brochu P, Pei Q. Advances in Dielectric Elastomers for Actuators and Artificial Muscles [J]. Macromolecular Rapid Communications, 2010, 31(1): 10–36.

[4] Pelrine R, Kornbluh R, Pei Q, et al. High-Speed Electrically Actuated Elastomers with Strain Greater Than 100% [J]. Science, 2000, 287(5454): 836–839.

[5] Ghevondyan M, Davtyan M, Aghayan M. Dielectric elastomer actuators: medical applications review [J]. Discover Materials, 2025, 5(1): 43.

[6] Biggs J, Danielmeier K, Hitzbleck J, et al. Electroactive Polymers: Developments of and Perspectives for Dielectric Elastomers [J]. Angewandte Chemie - International Edition, 2013, 52(36): 9409–9421.

[7] Pelrine R. Electrostriction of polymer dielectrics with compliant electrodes as a means of actuation [J]. Sensors & Actuators A Physical, 1998, 64(64): 77–85.

[8] Suo Z. Theory of dielectric elastomers [J]. Acta Mechanica Solida Sinica, 2010, 23(6): 549–578.

[9] Zhao X, Suo Z. Method to analyze electromechanical stability of dielectric elastomers [J]. Applied Physics Letters, 2007, 91(6): 061921-061921–3.

[10] Guo Y, Liu L, Liu Y, et al. Review of Dielectric Elastomer Actuators and Their Applications in Soft Robots [J]. Advanced Intelligent Systems, 2021, 3(10): 2000282.

[11] Lu T, Ma C, Wang T. Mechanics of dielectric elastomer structures: A review [J]. Extreme Mechanics Letters, 2020, 38: 100752.

[12] Stoyanov H, Kollosche M, Mccarthy D N, et al. Molecular composites with enhanced energy density for electroactive polymers [J]. Journal of Materials Chemistry, 2010, 20.

[13] Romasanta L J, Lopez-Manchado M A, Verdejo R. Increasing the performance of dielectric elastomer actuators: A review from the materials perspective [J]. Progress in Polymer Science, 2015, 51: 188–211.

[14] Gallone G, Carpi F, De Rossi D, et al. Dielectric constant enhancement in a silicone elastomer filled with lead magnesium niobate–lead titanate [J]. Materials Science and Engineering C, 2007, 27(1): 110–116.

[15] Carpi F, Gallone G, Galantini F, et al. Silicone–Poly(hexylthiophene) Blends as Elastomers with Enhanced Electromechanical Transduction Properties [J]. Advanced Functional Materials, 2008, 18(2): 235–241.

[16] Huang C, Zhang Q M, Su J. High-dielectric-constant all-polymer percolative composites [J]. Applied Physics Letters, 2003, 82(20): 3502–3504.

[17] Yang C, Lin Y, Nan C W. Modified carbon nanotube composites with high dielectric constant, low dielectric loss and large energy density [J]. Carbon, 2009, 47(4): 1096–1101.

[18] Dang Z, Yuan J, Yao S, et al. Flexible Nanodielectric Materials with High Permittivity for Power Energy Storage [J]. Advanced Materials, 2013, 25(44): 6334–6365.

[19] Jin L, Zhang C, Guo H, et al. Improved Electro-Actuation of Polydimethylsiloxane-Based Composite Dielectric Elastomer Via Constructing Semi-Interlocked Dual-Network [J]. 2024.

[20] Wang W, Ren G, Zhou M, et al. Preparation and Characterization of CCTO/PDMS Dielectric Elastomers with High Dielectric Constant and Low Dielectric Loss [J]. Polymers, 2021, 13(7): 1075.

[21] Wang Y, Jiang Y, Zang W, et al. A dual cone actuator with high energy density and long fatigue life by developing a nano-silica reinforced dielectric elastomer composite [J]. Composites Part A: Applied Science and Manufacturing, 2024, 180: 108039.

[22] Rong M Z, Zhang M Q, Zheng Y X, et al. Structure–property relationships of irradiation grafted nano-inorganic particle filled polypropylene composites [J]. Polymer, 2001, 42(1): 167–183.

[23] Zhang X, Shen Y, Xu B, et al. Giant Energy Density and Improved Discharge Efficiency of Solution-Processed Polymer Nanocomposites for Dielectric Energy Storage [J]. Advanced Materials, 2016, 28(10): 2055–2061.